Analytical Biochemistry 605 (2020) 113719

Contents lists available at ScienceDirect

Analytical Biochemistry

journal homepage: www.elsevier.com/locate/yabio

Nucleotide binding kinetics and conformational change analysis of tissue transglutaminase with switchSENSE

Regina Staffler[a], Ralf Pasternack[b], Martin Hils[b], Wolfgang Kaiser[a], Friederike M. Möller[a,*]

[a] Dynamic Biosensors GmbH, Lochhamer Str. 15, 82152, Martinsried, Germany
[b] Zedira GmbH, Roesslerstrasse 83, 64293, Darmstadt, Germany

ARTICLE INFO

Keywords:
Tissue transglutaminase
TG2
switchSENSE
Conformational changes
Kinetics
Inhibitors
Ligand binding assay
Biosensor
Protein structure

ABSTRACT

Function, activity, and interactions of proteins crucially depend on their three-dimensional structure and are often regulated by effector binding and environmental changes. Tissue transglutaminase (Transglutaminase 2, TG2) is a multifunctional protein, allosterically regulated by nucleotides and Ca^{2+} ions, which trigger opposing conformational changes. Here we introduce switchSENSE as a versatile tool for TG2 characterization and provide novel insights into protein conformation as well as analyte binding kinetics. For the first time, we succeeded in measuring the kinetic rate constants and affinities (k_{on}, k_{off}, K_D) for guanosine nucleotides (GMP, GDP, GTP, GTPγS). Further, the conformational changes induced by GDP, Ca^{2+} and the covalent inhibitor Z-DON were observed by changes in TG2's hydrodynamic diameter. We confirmed the well-known compaction by guanosine nucleotides and extension by Ca^{2+}, and provide evidence for TG2 conformations so far not described by structural analysis. Moreover, we analyze the influence of the peptidic Z-DON inhibitor and the R580A mutation on the conformational responsiveness of TG2 to its natural effectors. In summary, this work shows how the combination of structural and kinetic information obtained by switchSENSE opens new perspectives for the characterization of conformationally active proteins and their interactions with ligands, e.g. potential drug candidates.

1. Introduction

Human tissue transglutaminase (TG2) is an intra- and extracellularly localized, structurally and mechanistically complex protein. It fulfills multiple functions depending on its environment and is allosterically regulated by nucleotides and Ca^{2+} ions. Outside the cell, where Ca^{2+} levels are high, TG2's main function is protein crosslinking by transamidation [1,2], which plays a role in various biological mechanisms including matrix stabilization [3], cell differentiation [4], signaling [5–7], apoptosis [3], and cell-adhesion [8]. Intracellularly, at low Ca^{2+} levels, TG2 assumes GTPase [9] and G-Protein [3] functionality. TG2 consists of four domains - an N-terminal β-sandwich, a catalytic core and two C-terminal β-barrels [10,11]. Several intrinsically disordered regions allow for structural flexibility [12] and enable conformational changes, which regulate TG2 function. Measurements in solution with various methods like fluorescence anisotropy [13], capillary electrophoresis [14], FLIM-FRET [15], and small-angle-scattering [16] show that Ca^{2+} triggers TG2 into an extended conformation, while nucleotide binding stabilizes a compact state. These findings are supported by X-ray crystal structures. In 2002, the first crystal structure was obtained for the nucleotide bound compact state, which is also often called TG2s "closed" conformation [17]. In 2007, Pinkas et al. succeeded in crystallizing TG2 in an extended conformation after covalent binding of an irreversible, peptidic active site inhibitor [11]. Up to the present time, this structure is widely adapted to visualize the transamidating state of TG2, also referred to as active or "open" conformation even if essential calcium ions are missing.

TG2s structural diversity facilitates interactions with many different molecules, including proteins and small molecules. The N-terminal domain of TG2 strongly binds fibronectin, thus acting as an integrin-binding co-receptor which plays a role in cell migration [18,19]. Further, TG2 associates with heparin-sulfate chains of syndecan-4, playing a role in TG2-membrane trafficking and affecting its catalytic activity [20]. Guanosine nucleotides and Ca^{2+} are TG2s main conformational effectors. Ca^{2+} is known to interact with TG2, but little is known about the interaction parameters – not only the affinity but even the number of binding sites is still disputed [14,21]. For nucleotides, a single binding site was identified with K_D and IC_{50} measurements spanning the nM to μM range [10,22–25].

Due to its complex multifunctionality, its conformational flexibility,

* Corresponding author.
E-mail address: moeller@dynamic-biosensors.com (F.M. Möller).

https://doi.org/10.1016/j.ab.2020.113719
Received 20 December 2019; Received in revised form 17 February 2020; Accepted 3 April 2020
Available online 19 July 2020

and the extensive interaction network the mode of activation of TG2 is not yet fully understood and subject to current research. Nevertheless, TG2 is regarded as a promising therapeutic target, as it is suspected to play a role in various diseases, such as fibrosis, certain cancer types and neurodegenerative disorders [26]. The most prominent example for a pathophysiological state with TG2 involvement is celiac disease, in which the enzyme plays a dual role by breaking oral tolerance to gluten, and in addition constitutes the principal autoantigen [27,28]. Several reversible and irreversible inhibitors have been developed and patented [29,30]. However, so far only one TG2 inhibitor (ZED1227) has entered clinical trials (phase 2a) for the treatment of celiac disease (EudraCT Number 2017-002241-30).

Biophysical methods for the characterization of proteins and their interactions are widely used in research and drug development. Traditionally, these methods either aim to resolve structural features (e.g. nuclear magnetic resonance spectroscopy, X-ray crystallography, dynamic light scattering), or to measure (kinetic) interaction parameters (e.g. surface plasmon resonance (SPR), microscale thermophoresis (MST), isothermal calorimetry (ITC)). Currently, increasing effort is being made to combine these two worlds in order to understand the relation between binding interactions, molecular structure and activity, with the aim of shedding light on the mode of action of e.g. potential drug targets and therapeutic candidates [31]. switchSENSE is an emerging biophysical technology for the characterization of molecular interactions [32]. The measurement of kinetic interaction parameters (k_{on}, k_{off} K_D) and hydrodynamic protein size (D_H) is possible within the same assay by using time-resolved fluorescence readouts. The correlation of binding interaction and conformational change analyses enables structure-function relation studies for proteins and various ligands, such as small molecules, ions or peptides.

Fig. 1 shows a typical experimental workflow for the chip-based switchSENSE biosensor. Initially, the biochip carries short single stranded DNA nanolevers which are covalently attached to a gold electrode on one end and modified with a fluorescent dye on the other end. The target protein is immobilized on the sensor surface by hybridization of pre-prepared target protein-ssDNA conjugates with the complementary DNA sequence. To regenerate the chip, the double stranded DNA nanolevers are denatured by disrupting the hydrogen bonds between base pairs using a high-pH regeneration solution. The conjugate is washed away while the covalently attached single-stranded nanolevers remain on the surface and can be reused for a new functionalization step.

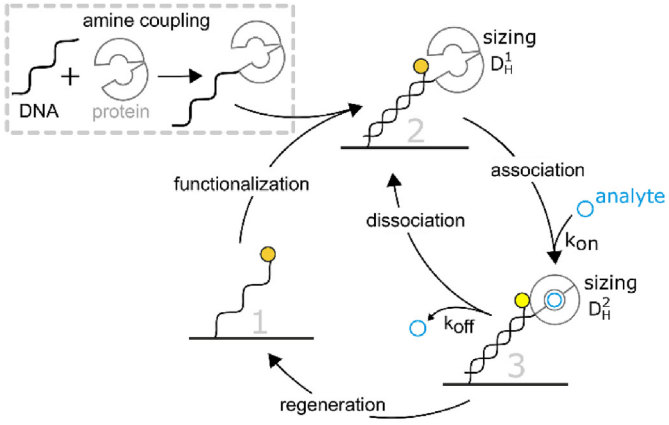

Fig. 1. switchSENSE measurement workflow. Initially, the switchSENSE biochip carries covalently attached fluorescently labeled ssDNAs (1). To functionalize the sensor with the protein of interest (here TG2), target protein-DNA conjugates are hybridized to the chip (1 → 2). These conjugates are pre-prepared using standard chemistry, such as amine coupling (dashed box). Association and dissociation kinetics (2 → 3 → 2) of analytes (here nucleotides) yield rate constants (k_{on}, k_{off}). Protein sizing (2, 3) in the presence or absence of analytes yields hydrodynamic diameters D_H and allows assessing conformational changes. The chip can be easily regenerated by breaking the DNA double strands using high pH regeneration solution (3 → 1), which allows the reuse of the chip multiple times.

Two different measurement modes are available for protein(-interaction) characterization. In the dynamic mode, alternating potentials are applied to the gold electrode and the nanolevers are swayed through solution. The motion of the nanolevers is tracked in real time by time-resolved single photon counting. The speed of the motion depends on the size of the protein attached to the DNA nanolevers, which allows the determination of the hydrodynamic diameter (D_H) of the immobilized protein [32,33] - in the present study of TG2. Changes in D_H upon exposure to effectors (such as small molecules or ions) provide information on conformational changes, such as domain movements or "stiffening" of flexible domains.

In the so-called static mode, a constant negative potential is applied to the electrode and binding kinetics are observed as changes in fluorescence emission. These changes reflect the physico-chemical changes in the local environment of the fluorophore, for instance of local hydrophobicity, caused by analyte binding.

Here, we apply switchSENSE to resolve the interaction kinetics (k_{on}, k_{off} and K_D) between TG2 and four different guanosine nucleotides (GMP, GDP, GTP, GTPγS). Furthermore, we report on the conformational response of TG2 to Ca^{2+} and guanosine nucleotides and evaluate the structural effects of the irreversible TG2-inhibitor Z-DON.

2. Materials and methods

2.1. Materials

Wildtype human transglutaminase 2 (TG2, recombinantly produced in insect cells (T022), HEK-293F cells (T034) and *E. coli* (T002)), and its Arg580Ala-mutant (TG2-R580A, recombinantly produced in *E. coli* cells, T169) were obtained from Zedira (Darmstadt, Germany). If not explicitly stated differently in the main text, wildtype TG2 recombinantly produced in insect cells was used. Also, the synthetic TG2 inhibitor Z-DON (benzyloxycarbonyl-(6-diazo-5-oxonorleucinyl)-L-valinyl-L-prolinyl-L-leucinmethylester, Z006) was provided by Zedira (Darmstadt, Germany). "DON" compounds are side chain modified peptides, with an electrophilic DON (6-diazo-5-oxonorleucinyl) group, which are potent and irreversible blockers of transglutaminase's cross-linking activity. Guanosine 5′-monophospate disodium salt hydrate (GMP), guanosine 5′-diphosphate sodium salt (GDP), guanosine 5′-triphosphate sodium salt (GTP) and guanosine 5′-O-(3-thiotriphosphate) (GTPγS) were purchased at Sigma Aldrich, dissolved in water and stored at −80 °C. The solutions were freshly thawed and diluted in measurement buffer for every experiment. All measurements were performed in switchSENSE standard buffer TE40 with 0.1 mM TCEP (10 mM Tris-HCl pH 7.4, 40 mM NaCl, 50 μM EDTA, 50 μM EGTA, 0.05% Tween20, 0.1 mM TCEP (tris(2-carboxyethyl)phosphine)), which allows for hydrodynamic diameter measurements. TCEP was added to the buffer to protect TG2 from oxidization. In contrast to classical G-proteins TG2 does not require Mg^{2+} for nucleotide binding [34]. Moreover, TG2 transamidation activity is inhibited by Mg^{2+} [35]. Therefore, all experiments were performed in the absence of Mg^{2+}, if not explicitly stated differently.

2.2. switchSENSE

2.2.1. Preparation of Protein-DNA conjugates

TG2 and its R580A mutant were covalently coupled via their primary amines, e.g. NH_2-terminus or lysine side chains to the 5' end of ssDNA (cNL-B48) (coupling kit CK-NH2-1-B48, Dynamic Biosensors, Martinsried, Germany). Protein-DNA conjugates were separated from free DNA and free protein using anion exchange chromatography. The corresponding chromatograms can be found in the Supplementary Information (SI 1). The conjugates elute in single, well-separable peaks,

which points at one-to-one labeling. Experience with several other proteins showed that conjugates with multiple DNAs attached elute later than a single-DNA conjugate and appear as separate peaks in the anion exchange chromatogram (data not shown). After liquid nitrogen freezing, the conjugates were stored at a concentration of 400 nM in TE40 buffer (10 mM Tris-HCl pH 7.4, 40 mM NaCl, 50 μM EDTA, 50 μM EGTA, 0.05% Tween20) at −80 °C and were freshly thawed before each experiment. 250 μg of protein yielded enough conjugate for more than 400 hybridizations corresponding to a conjugation yield of 50%.

2.2.2. Chip functionalization

All switchSENSE experiments were performed on a yellow single-color DRX instrument using a standard switchSENSE chip (MPC-48-2-Y1, Dynamic Biosensors), which carries covalently attached fluorescently labeled ssDNA. The proteins (TG2, TG2-R580) were immobilized on the biochip via hybridization of complementary DNA-protein conjugates. The chip was regenerated and freshly functionalized before each measurement series. For chip regeneration, the double stranded DNA nanolevers were denatured by disrupting the hydrogen bonds between base pairs using a high-pH regeneration solution (SOL-REG-12- 1, Dynamic Biosensors). Subsequently, the conjugate was washed away while the covalently attached single-stranded nanolevers remained on the surface and could be reused for a new functionalization step.

2.2.3. Nucleotide binding kinetics

Nucleotide binding kinetics were measured in switchSENSE's static mode. After functionalization of the nanolevers with the protein of interest (TG2, TG2-R580A), association and dissociation curves were measured for at least 5 different analyte concentrations by alternatingly injecting increasing concentrations of analyte solution (association) and buffer (dissociation). The fluorescence traces were analyzed with the switchANALYSIS software (Dynamic Biosensors GmbH, Germany) by fitting all association and dissociation curves of one dataset (at least 5 different analyte concentrations) simultaneously (global fit) by using a simple fit model for one-to-one interactions. The association curves were fitted by $f_{assoc}(t, c) = a(c)\cdot[1 - \exp(-k_{on}^{obs} t)]$, with the concentration-dependent observed on rate $k_{on}^{obs} = c\cdot k_{on} + k_{off}$ and signal amplitude a. The dissociation curves were fitted by $f_{diss}(t, c) = a\cdot\exp(-k_{off} t)]$. The extremely fast association rate constants on the order of 10^7 $M^{-1}s^{-1}$ require special measures to avoid artifacts from mass transport limitation and rebinding. This entails choosing a high flowrate of 2000 μL/min to ensure solution exchange in the microsecond timescale, a high sampling rate of 10 Hz and comparably low surface densities of approximately 200 molecules per μm^2 (equivalent to ≈ 10 resonance units in SPR).

2.2.4. Conformational change measurements

Hydrodynamic protein diameters (D_H) were measured using switchSENSE's dynamic mode according to the method described earlier [32]. Protein sizing was performed directly after chip functionalization in measurement buffer and after exposure to various effectors. Effector concentrations well above the K_D were chosen ($c_{GDP,GTP,GTP\gamma S}$ = 500 nM, c_{GMP} = 200 μM, c_{Ca2+} = 500 μM, $c_{Z\text{-}DON}$ = 100 μM). The concentrations for the Z-DON inhibitor and Ca^{2+} were estimated based on literature values (IC_{50}^{Z-DON} = 20 nM [36], K_D^{Ca2+} = 0.15–5 μM [24,37]). It should be noted that these concentrations were not chosen to reflect physiological conditions, but to ensure that all proteins on the surface were in the effector-bound state and adopted the same conformation.

Conformational changes are reported as relative size changes compared to the measured initial protein size after chip functionalization. The reported values represent mean values with standard deviation from at least 3 independent runs. In some runs the absolute sizes showed a deviation from the mean of up to 2.6 nm (38%), while relative size changes were highly reproducible (variation < 4%). The reason could be dimerization, self-crosslinking or disulfide formation during storage, thawing or exposure to electric fields. Along this line, earlier studies found that disulfide formation decreases TG2s ability to assume a compact conformation upon GTP exposure [10]. TG2 aging was also observable on the chip with TG2's size drifting over time on the chip (≈3% within 4 buffer injections with sizing, data not shown). In order to limit oxidization to a minimum, all measurements were performed under reducing conditions with measurement buffer containing 0.1 mM TCEP.

3. Results and discussion

3.1. Nucleotide binding kinetics

The interactions between TG2 and various nucleotides have been studied in the past mostly by activity assays and equilibrium methods, such as ITC. Equilibrium methods yield the dissociation constant K_D of an interaction, which describes the concentration of analyte at which half of all binding sites are occupied. The K_D is a valuable measure for the strength of an interaction. However, in order to fully understand an interaction, it is also important to determine binding kinetics, i.e. to learn how fast the interaction happens and how stable it is.

Here, we resolve the binding kinetics between nucleotides and TG2 for the first time and determine the kinetic rate constants (k_{on}, k_{off}) and dissociation constant (K_D) for the four guanosine nucleotides GMP, GDP, GTP and GTPγS. The binding of these nucleotides to immobilized TG2 on the sensor surface was observed in switchSENSE's static mode by an increase in fluorescence on a timescale of a few seconds.

To resolve the extremely fast binding kinetics, a high flow rate of 2000 μL/min was applied, which enabled solution exchange within milliseconds. Examples of association and dissociation curves for the four nucleotides are shown in Fig. 2A. Each kinetic dataset was globally fitted with a monoexponential fit model yielding k_{on}, and k_{off}. The averaged fit parameters (k_{on}, k_{off}) and the resulting K_D ($K_D = k_{off}/k_{on}$) from three independent runs with at least 5 different concentrations are listed in Table 1 and are visually compared in the rate map in Fig. 2B.

We identified GMP as by far the weakest binder out of the four tested nucleotides with a K_D of 3.6 ± 1.6 μM. GDP already shows a 400 fold tighter binding with a K_D of 8.7 ± 4.5 nM. Only slightly tighter binding was observed for GTP (2.4 ± 0.7 nM) and its non-hydrolyzable analog GTPγS (1.2 ± 0.2 nM). The ranking of affinities agrees with observations from activity assays and structural considerations [21,38], and can be explained by the increasing number of electrostatic interactions and hydrogen bonds per phosphate group [24]. IC_{50} values for GTPγS, GTP and GDP have typically been measured in the low μM range [10,23,39], while inhibition by GMP was found to required much higher concentrations [23]. In contrast to activity assay results, direct reports on binding affinities are rather rare. Murthy et al. estimated GDP/GTP affinities of 25 nM using fluorescent nucleotide analogs [22]. Using a similar approach, Datta et al. quantified K_Ds for GDP and GTPγS as 1.5 μM and 320 nM, respectively. In both cases the fluorescence modifications are likely to influence the interaction. Equilibrium measurements with unmodified nucleotides using isothermal calorimetry (ITC) were reported by Begg et al. [40]. However, the determined value of 1.6 μM should rather be regarded as an upper limit, due to the high protein concentration used in the measurements to achieve a satisfying signal-to-noise ratio. To our knowledge, kinetic rate constants that compare with our results have not been reported yet.

A closer look at the rate map reveals, that the low affinity for GMP in comparison to the other nucleotides is predominantly due to a drastically slower on-rate. The second phosphate group appears to be important for the recognition by TG2. While the binding of GDP, GTP and GTPγS proceeds extremely rapidly with similar k_{on}s on the order of 10^7 $M^{-1}s^{-1}$, GMP binding is 3 orders of magnitude slower. When examining the plots in Fig. 2A, the large difference at first sight is

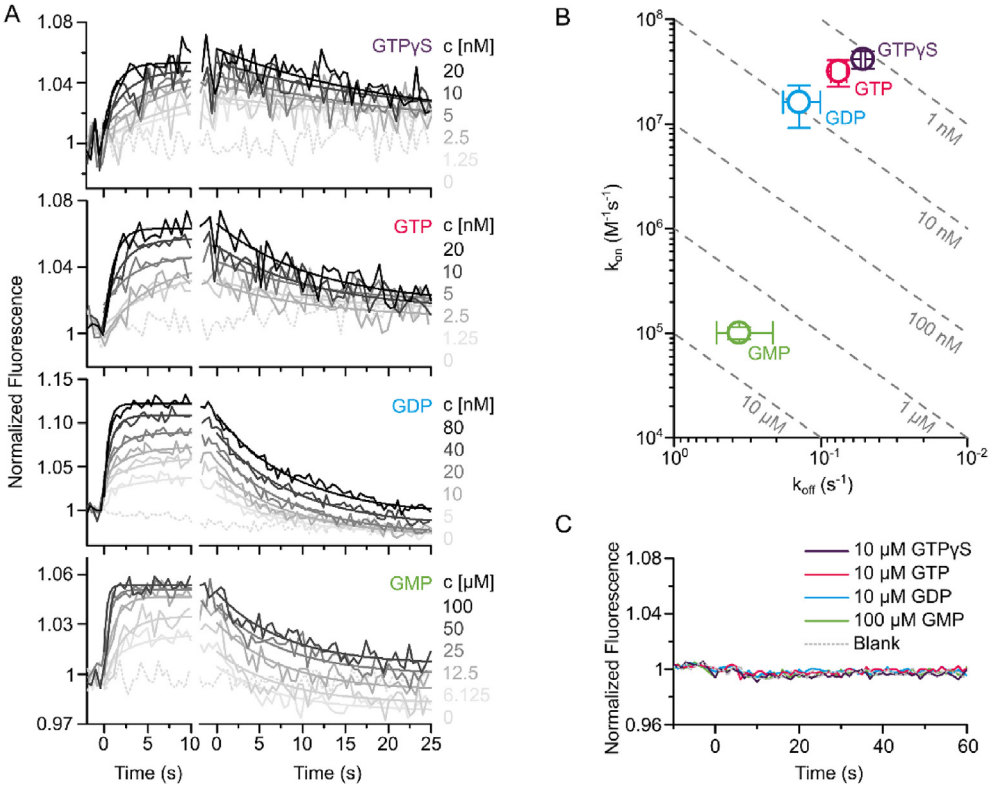

Fig. 2. A Examples of kinetics between wildtype TG2 and four different nucleotides observed via fluorescence changes upon analyte binding and release. Smooth solid lines are fits obtained by global fitting. Note that GMP concentrations are 3 orders of magnitude higher than for the other nucleotides. **B** Rate map representation of k_{on} and k_{off}. Error bars represent the standard deviation from at least 3 independent runs. Lines of constant K_D are shown as dashed lines. **C** Injections of nucleotides to the nucleotide binding deficient R580A TG2 mutant do not affect fluorescence, verifying specificity of the signals observed in panel A.

Table 1
Average association rate (k_{on}), dissociation rate (k_{off}) and dissociation constant (K_D) values from three independent runs with respective standard deviations.

	$k_{on}/10^6$ $M^{-1}s^{-1}$	$k_{off}/10^{-2}$ s^{-1}	K_D/nM
GTPγS	41 ± 8	5.1 ± 0.2	1.2 ± 0.2
GTP	32 ± 9	7.6 ± 1.0	2.4 ± 0.7
GDP	16 ± 7	14 ± 4	8.7 ± 4.5
GMP	0.10 ± 0.01	36 ± 15	3600 ± 1600

surprising, considering that the kinetics for GMP do not look too much different, with a comparable observed association timescale τ_{assoc}. This time scale does not directly report on the intrinsic on-rate k_{on}, though, but also depends on the off-rate and the applied nucleotide concentrations ($\tau_{assoc} = 1/k_{obs}$ with $k_{obs} = k_{on} \cdot c + k_{off}$). Hence, interactions with very different k_{on}s can show comparable association curves, if different analyte concentrations are used for kinetic measurements. This is the case here, where the highest GMP concentration is approximately 1000-fold higher than that used for the other nucleotides.

In contrast to the association rate constants, the dissociation rate constants for all tested nucleotides including GMP vary only within one order of magnitude. Thereby, the dissociation rate is subtly slower, the more phosphates are present. Interestingly, GTPγS dissociates almost as fast as the other nucleotides, indicating that hydrolysis is not required for release from TG2, in contrast to the findings of Raw et al. on the behavior of other G-proteins [41].

All kinetics were measured in switchSENSE's static mode by monitoring fluorescence changes in real time. Besides binding-induced fluorescence shifts, the fluorophore could also respond unspecifically to changes in buffer composition, e.g. ionic strength variation. To ensure specificity of the observed binding signals, all analytes were also allowed to flow across an unfunctionalized reference electrode without protein and no signal changes were observed (SI 2). As another control, we also tested the response of the R580A mutant of TG2, which is lacking the ability to bind nucleotides [10,42]. As shown in Fig. 2C, the resulting fluorescence trace remained flat even at high nucleotide concentrations.

The successful measurement of nucleotide binding kinetics raised the hope of also resolving Ca^{2+} and inhibitor binding kinetics. Unfortunately, Ca^{2+} injections resulted in a strong unspecific fluorescence response, concealing any specific binding signal. In contrast, injections of the irreversible-acting inhibitor Z-DON did not result in any fluorescence change with or without Ca^{2+} in the measurement buffer. We anticipate that with advanced assay development we will be able to resolve the direct binding of Ca^{2+} and Z-DON using switchSENSE in future. Promising strategies include the development of competition assays with (fluorescent) compounds and the use of different fluorophores, e.g. less ionic strength dependent dyes to unmask the specific Ca^{2+} binding signal, or dyes which are more sensitive to physico-chemical changes in their environment to reveal Z-DON binding by enhancing the fluorescence response.

3.2. GDP and Ca^{2+} induced conformational changes

The function of TG2 is known to be regulated by its conformation, which is affected by the antagonistic effectors GDP/GTP and Ca^{2+}. The determination of hydrodynamic diameters on a chip allows the investigator to observe conformational changes dynamically. The very same proteins can be exposed sequentially and repeatedly to various effectors.

Fig. 3A shows the results from three different effector exposure sequences and provides insights into the conformational effects on TG2 and their reversibility. The effects of the conformational effectors are reported as relative size changes with respect to TG2's hydrodynamic diameter in the absence of effectors, which was always measured in running buffer (TE40 + 0.1 mM TCEP) directly after chip functionalization. Before injection of a new effector, the flow channel was routinely washed with EGTA/EDTA-containing running buffer to fully remove any previous effectors.

In each of the three measurement sequences, GDP was injected after determination of the initial hydrodynamic diameter, and a consistent decrease in TG2s hydrodynamic diameter by 14 ± 3% was observed.

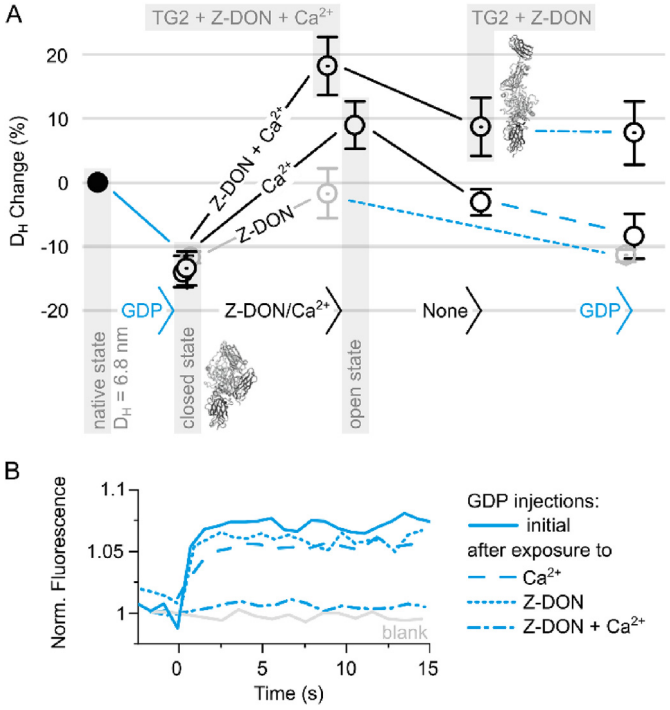

Fig. 3. A Hydrodynamic diameter (D_H) changes of TG2 in response to sequentially applied effectors, normalized to the initial "naïve" D_H after chip functionalization in absence of any effector. The average D_H of this naïve state was found to be 6.8 ± 0.8 nm. 500 nM GDP induced a D_H decrease, while 500 μM Ca^{2+} had the opposite effect. Both changes were fully reversible, as TG2 readopted its initial size after removal of both effectors. When TG2 was exposed to 100 μM Z-DON together with 500 μM Ca^{2+}, an even larger D_H increase was observed. Subsequently, TG2s initial size was not recovered after washing, and compaction by GDP was suppressed, indicating an irreversible effect of Z-DON on conformation. None of these effects was observed when TG2 was exposed to Z-DON in the absence of Ca^{2+}. **B**: GDP binding kinetics. Line appearances correspond to panel A. GDP binding was observed after exposure to Ca^{2+} and Z-DON alone, but not when Z-DON was applied together with Ca^{2+}.

Comparable compaction was also measured for GMP, GTP and GTPγS (see SI3). The next size measurement in sequence 1 (Fig. 3A, symbol ○) was performed in the presence of 500 μM Ca^{2+}. In agreement with the literature [13], Ca^{2+} had an opposite effect to that of GDP and induced a D_H increase by 9 ± 3%. The further course of this measurement sequence demonstrates the full reversibility of the induced conformational changes: TG2 readopted its initial size after washing with EGTA-containing buffer and repeated GDP exposure induced re-compaction.

Interestingly, these results also show that TG2 reproducibly assumes an intermediate size in the absence of any effectors, which suggests two interpretations: either TG2 adopts a still undescribed naïve conformation or the TG2 population on the chip is heterogenous with both "open" and "closed" conformations present. Solving this ambiguity remains to be elucidated in future research.

To determine whether the measured Ca^{2+}-induced protein size increase indeed reflects a conformational change and is not an ionic-strength related artifact, we performed a control experiment in which Ca^{2+} was replaced by Mg^{2+}. In contrast to Ca^{2+}, Mg^{2+} does not "push" TG2 into its open conformation [14], while still having the same effect on the ionic strength. We observed that TG2's hydrodynamic diameter is not influenced by Mg^{2+} (ΔD_H = 3 ± 3%) confirming that the influence of ionic strength on protein size is negligible and that the Ca^{2+} induced size increase specifically indicates a conformational change.

The second and third measurement sequences in Fig. 3A address the influence of the potent, irreversible and site-specific inhibitor Z-DON on TG2 conformation and its responsiveness to GDP and Ca^{2+}. Z-DON is a side chain modified peptide which irreversibly binds to TG2's substrate binding site, leading to an irreversible alkylation of TG2's active site. The simultaneous incubation of TG2 with Ca^{2+} and Z-DON (symbol ⊙) increased TG2's size by 18 ± 4%, which exceeded the size increase produced by Ca^{2+} alone by a factor of 2. After removal of Ca^{2+}, TG2 did not regain its initial size. Instead it adopted a state with a size comparable to TG2 without inhibitor, but in the presence of Ca^{2+}. Previously, the comparable hydrodynamic sizes of these two states were used to argue that the crystal structure of the open conformation (binary complex of TG2 and an irreversible peptidic inhibitor in the absence of Ca^{2+}) corresponds to the TG2-Ca^{2+} binary complex conformation [11]. Our findings show that the TG2-Ca^{2+} complex rather adopts a different conformation, which has so far escaped structural analysis. Thereby our results experimentally confirm SAXS/SANS based Monte Carlo simulations of the gyration radius in the absence and presence of various effectors [16], and support the idea that the crystallized open TG2 conformation looks like an inert molecule and might not correspond to the active Ca^{2+}-bound conformation [21].

This sequence further shows that covalent binding of the Z-DON inhibitor only partially limits the conformational flexibility of TG2. After inhibitor binding in the presence of Ca^{2+}, removal of Ca^{2+} caused a size decrease, while subsequent exposure to GDP had no impact on protein size. The GDP induced conformational change is suppressed in agreement to the literature findings [11], while the conformational responsiveness to Ca^{2+} is retained, which indicates that the conformational dynamics of TG2 are governed by multiple (at least two) mechanisms.

None of these Z-DON induced effects became apparent when TG2 was exposed to the inhibitor in the absence of Ca^{2+} (⊙). Z-DON alone did not induce a size increase beyond that exhibited by the buffer alone, and GDP-induced compaction was still observed. Taken together these data confirm that TG2 requires Ca^{2+} to react with Z-DON, as expected. The fluorescence kinetics in Fig. 3B support this interpretation. The characteristic fluorescence increase upon GDP injection was observed for the GDP binding steps in Fig. 3A, which were preceded by exposure to Ca^{2+}, buffer and/or Z-DON alone. However, after exposure to Z-DON in the presence of Ca^{2+} the fluorescence remained at a baseline level.

The conformational change behavior of TG2 as determined by switchSENSE qualitatively agrees with literature (where available). Interestingly the measured absolute hydrodynamic diameters appear smaller than expected, though. For example, structure-based D_H calculations and dynamic light scattering measurements for the two crystallized TG2 states yielded diameters of about 7.4 nm (PDB 1KV3) for the GDP-bound compact state and 8.1 nm in the inhibitor bound state in the absence of Ca^{2+} (PDB 3S3J) [11], while we measured values of 5.9 ± 0.6 nm and 7.0 ± 0.4 nm, respectively. A complete list of measured absolute D_H values for all analyzed TG2 states can be found in the Supplementary Information. We argue that the deviations might be due to the anchoring of TG2 on the chip surface and the peculiar structure of TG2, which might rather resemble a "string of pearls" than a rigid structure. switchSENSE measurements on a different protein with disordered regions showed, that the measured absolute size varied depending on the DNA coupling site without compromising conformational change detection (data not shown). For this protein, the amplitude of the size change increased when the coupling site moved closer to the conformational active site. In future studies on TG2, it would be interesting to determine how site-specific coupling to different domains of TG2 would influence the absolute hydrodynamic diameter measurements and the conformational change detection. Such results could probably yield insights into the involvement of the different domains during effector induced conformational changes. Site specific labeling of TG2 could, for example, be achieved by enzymatic labeling using microbial transglutaminase [43,44] or sortase [45].

We also investigated the conformational response of the TG2-R580A mutant to GDP and Ca^{2+}. As the available mutant protein was produced in *E. coli* cells while the wildtype protein used in the present

work was produced in insect cells, we first ruled out the possibility that potentially different posttranslational modifications influence conformational change measurements. To this end, we measured the GDP and Ca^{2+} induced conformational changes in wildtype TG2 recombinantly produced in HEK, *E. coli* and insect cells, and observed comparable behavior (see SI 4). For the mutant we observed that its size remained constant when exposed to GDP, while a size increase of 17 ± 3% was observed in the presence of Ca^{2+}. These findings correlate with literature findings showing that the mutant cannot bind GDP, but still shows transamidase activity – a function associated with Ca^{2+} binding [42]. A FLIM-FRET study showed that the R580A mutant adopts an open-like structure with C and N termini far apart [15]. Interestingly though, the TG2 R580A mutant appeared to be significantly smaller (D_H = 5.1 ± 0.3 nm) than the wild type enzyme (D_H = 6.8 ± 0.8 nm) in the switchSENSE assay. As pointed out above, a decrease in hydrodynamic diameter can, on the one hand, provide information on compaction due to a domain movement, and, on the other hand, equally well on increased flexibility, e.g. due to an increased proportion of disordered regions. Here, the combination of FLIM-FRET data and switchSENSE results points towards the second explanation.

4. Conclusions

The regulation of transglutaminases' protein crosslinking activity is of outmost importance for drug development in order to specifically target the activity when and where required, while at the same time avoiding secondary physiological effects. Negative regulation by purine nucleotides protects against unsolicited transglutaminase activity within cells.

In recent years, the importance of kinetic characterization of drugs in contrast to equilibrium-based affinity and activity assays has been more and more appreciated for drug discovery [46,47]. Here, we report kinetic rate constants for four guanosine nucleotides binding to TG2, revealing fast association and dissociation rate constants for GDP, GTP and GTPγS, and strongly reduced affinity and on-rate for GMP. Conformational change analyses showed that all nucleotides "push" TG2 into its compact, closed state, while Ca^{2+} triggers an extended form of TG2 prone to react with the mechanism-based Z-DON inhibitor. Hydrodynamic diameter measurements allow easy discrimination of the ternary TG2-Ca^{2+}-Inhibitor complex from the binary ones, e.g. TG2-Ca^{2+} and TG2-inhibitor complexes. Although the latter two exhibited the same size, the dynamic exchange of effectors allows one to discriminate between them based on their different conformational responsiveness to GDP. These data suggest that there is at least one relevant TG2 conformation (TG2-Ca^{2+}) that has escaped X-ray crystal structure analysis so far.

In conclusion, the switchSENSE experiments have elegantly confirmed well known conformational effects, and experimentally proved simulations and structural considerations. Further, the platform has provided the first report on nucleotide binding kinetics. Thereby we introduce switchSENSE as a valuable platform technology to identify yet unknown TG2 modulators. Either classical small-molecules or antibodies/antibody fragments stabilizing certain conformational states could be characterized and identified as potential drug candidates or as tool compounds to decipher the multifaceted TG2 functions.

Author contributions

Regina Staffler: Investigation, Formal Analysis, Writing - Review & Editing, Visualization.

Martin Hils: Writing - Review & Editing.

Ralf Pasternack: Writing - Review & Editing.

Wolfgang Kaiser: Supervision.

Friederike M Möller: Conceptualization, Formal Analysis, Writing - Original Draft, Visualization, Supervision.

Declaration of competing interest

F.M., R.S. and W.K are/were employees of Dynamic Biosensors GmbH, W.K. is one of the founders of Dynamic Biosensors. R.P. and M.H. are shareholders/employees at Zedira.

Acknowledgements

The authors gratefully acknowledge Andreas Heil, Martin Stieler, Christian Büchold and Ulrich Rant for fruitful discussions and Fjolla Ismajli for technical support with the preparation of protein-DNA conjugates. This research did not receive any specific grant from funding agencies in the public, commercial, or not-for-profit sectors.

Appendix A. Supplementary data

Supplementary data to this article can be found online at https://doi.org/10.1016/j.ab.2020.113719.

References

[1] L. Lorand, R.M. Graham, Transglutaminases: crosslinking enzymes with pleiotropic functions, Nat. Rev. Mol. Cell Biol. 4 (2003) 140–156, https://doi.org/10.1038/nrm1014.

[2] M. Griffin, R. Casadio, C.M. Bergamini, Transglutaminases: nature's biological glues, Biochem. J. 368 (2002) 377–396, https://doi.org/10.1042/bj20021234.

[3] Z. Sarang, P. Molnár, T. Németh, S. Gomba, T. Kardon, G. Melino, S. Cotecchia, L. Fésüs, Z. Szondy, Tissue transglutaminase (TG2) acting as G protein protects hepatocytes against Fas-mediated cell death in mice, Hepatology 42 (2005) 578–587, https://doi.org/10.1002/hep.20812.

[4] Z. Balajthy, Tissue-transglutaminase contributes to neutrophil granulocyte differentiation and functions, Blood 108 (2006) 2045–2054, https://doi.org/10.1182/blood-2004-02-007948.

[5] H. Nakaoka, D. Perez, K. Baek, T. Das, A. Husain, K. Misono, M. Im, R. Graham, G_h: a GTP-binding protein with transglutaminase activity and receptor signaling function, Science 264 (1994) 1593–1596, https://doi.org/10.1126/science.7911253.

[6] R. Vezza, A. Habib, G.A. FitzGerald, Differential signaling by the thromboxane receptor isoforms via the novel GTP-binding protein, G_h*, J. Biol. Chem. 274 (1999) 12774–12779, https://doi.org/10.1074/jbc.274.18.12774.

[7] L.K. Boroughs, M.A. Antonyak, R.A. Cerione, A novel mechanism by which tissue transglutaminase activates signaling events that promote cell survival, J. Biol. Chem. 289 (2014) 10115–10125, https://doi.org/10.1074/jbc.M113.464693.

[8] S.S. Akimov, D. Krylov, L.F. Fleischman, A.M. Belkin, Tissue Transglutaminase is an integrin-binding adhesion coreceptor for fibronectin, J. Cell Biol. 148 (2000) 825–838, https://doi.org/10.1083/jcb.148.4.825.

[9] K.N. Lee, P.J. Birckbichler, M.K. Patterson, GTP hydrolysis by Guinea pig liver transglutaminase, Biochem. Biophys. Res. Commun. 162 (1989) 1370–1375, https://doi.org/10.1016/0006-291X(89)90825-5.

[10] G.E. Begg, P.H. Stokes, J.M. Matthews, M.A. Wouters, A. Husain, L. Lorand, S.E. Iismaa, R.M. Graham, Mechanism of allosteric regulation of transglutaminase 2 by GTP, Proc. Natl. Acad. Sci. Unit. States Am. 103 (2006) 19683–19688.

[11] D.M. Pinkas, P. Strop, A.T. Brunger, C. Khosla, Transglutaminase 2 undergoes a large conformational change upon activation, PLoS Biol. 5 (2007) e327.

[12] K. Kanchan, M. Fuxreiter, L. Fésüs, Physiological, pathological, and structural implications of non-enzymatic protein–protein interactions of the multifunctional human transglutaminase 2, Cell. Mol. Life Sci. 72 (2015) 3009–3035, https://doi.org/10.1007/s00018-015-1909-z.

[13] A. Di Venere, A. Rossi, F. De Matteis, N. Rosato, A.F. Agrò, G. Mei, Opposite effects of Ca^{2+} and GTP binding on tissue transglutaminase tertiary structure, J. Biol. Chem. 275 (2000) 3915–3921.

[14] C.M. Clouthier, G.G. Mironov, V. Okhonin, M.V. Berezovski, J.W. Keillor, Real-time monitoring of protein conformational dynamics in solution using kinetic capillary electrophoresis, Angew. Chem. Int. Ed. 51 (2012) 12464–12468, https://doi.org/10.1002/anie.201205575.

[15] N.S. Caron, L.N. Munsie, J.W. Keillor, R. Truant, Using FLIM-FRET to measure conformational changes of transglutaminase type 2 in live cells, PloS One 7 (2012) e44159, , https://doi.org/10.1371/journal.pone.0044159.

[16] P. Mariani, F. Carsughi, F. Spinozzi, S. Romanzetti, G. Meier, R. Casadio, C.M. Bergamini, Ligand-induced conformational changes in tissue transglutaminase: Monte Carlo analysis of small-angle scattering data, Biophys. J. 78 (2000) 3240–3251.

[17] S. Liu, R.A. Cerione, J. Clardy, Structural basis for the guanine nucleotide-binding activity of tissue transglutaminase and its regulation of transamidation activity, Proc. Natl. Acad. Sci. Unit. States Am. 99 (2002) 2743–2747.

[18] S.S. Akimov, A.M. Belkin, Cell surface tissue transglutaminase is involved in adhesion and migration of monocytic cells on fibronectin, Blood 98 (2001) 1567–1576, https://doi.org/10.1182/blood.V98.5.1567.

[19] I. Cardoso, E.C. Østerlund, J. Stamnaes, R. Iversen, J.T. Andersen, T.J.D. Jørgensen, L.M. Sollid, Dissecting the interaction between transglutaminase 2 and fibronectin,

Amino Acids 49 (2017) 489–500, https://doi.org/10.1007/s00726-016-2296-y.
[20] A. Scarpellini, R. Germack, H. Lortat-Jacob, T. Muramatsu, E. Billett, T. Johnson, E.A.M. Verderio, Heparan sulfate proteoglycans are receptors for the cell-surface trafficking and biological activity of transglutaminase-2, J. Biol. Chem. 284 (2009) 18411–18423, https://doi.org/10.1074/jbc.M109.012948.
[21] R. Király, M. Demény, L. Fésüs, Protein transamidation by transglutaminase 2 in cells: a disputed Ca^{2+}-dependent action of a multifunctional protein, FEBS J. 278 (2011) 4717–4739, https://doi.org/10.1111/j.1742-4658.2011.08345.x.
[22] S.P. Murthy, L. Lorand, Nucleotide binding by the erythrocyte transglutaminase/Gh protein, probed with fluorescent analogs of GTP and GDP, Proc. Natl. Acad. Sci. Unit. States Am. 97 (2000) 7744–7747.
[23] T.-S. Lai, T.F. Slaughter, K.A. Peoples, J.M. Hettasch, C.S. Greenberg, Regulation of human tissue transglutaminase function by magnesium-nucleotide complexes: identification of distinct binding sites for Mg-GTP and Mg-ATP, J. Biol. Chem. 273 (1998) 1776–1781, https://doi.org/10.1074/jbc.273.3.1776.
[24] C.M. Bergamini, A. Dondi, V. Lanzara, M. Squerzanti, C. Cervellati, K. Montin, C. Mischiati, G. Tasco, R. Collighan, M. Griffin, R. Casadio, Thermodynamics of binding of regulatory ligands to tissue transglutaminase, Amino Acids 39 (2010) 297–304, https://doi.org/10.1007/s00726-009-0442-5.
[25] S. Datta, M.A. Antonyak, R.A. Cerione, Importance of Ca^{2+}-dependent transamidation activity in the protection afforded by tissue transglutaminase against doxorubicin-induced apoptosis, Biochemistry 45 (2006) 13163–13174, https://doi.org/10.1021/bi0606795.
[26] Z. Szondy, I. Korponay-Szabó, R. Király, Z. Sarang, G.J. Tsay, Transglutaminase 2 in human diseases, Biomedicine 7 (2017) 15, https://doi.org/10.1051/bmdcn/2017070315.
[27] B. Fleckenstein, Ø. Molberg, S.-W. Qiao, D.G. Schmid, F. von der Mülbe, K. Elgstøen, G. Jung, L.M. Sollid, Gliadin T cell epitope selection by tissue transglutaminase in celiac disease, J. Biol. Chem. 277 (2002) 34109–34116, https://doi.org/10.1074/jbc.M204521200.
[28] L.M. Sollid, The roles of MHC class II genes and post-translational modification in celiac disease, Immunogenetics 69 (2017) 605–616, https://doi.org/10.1007/s00251-017-0985-7.
[29] J.W. Keillor, K.Y.P. Apperley, A. Akbar, Inhibitors of tissue transglutaminase, Trends Pharmacol. Sci. 36 (2015) 32–40, https://doi.org/10.1016/j.tips.2014.10.014.
[30] J.W. Keillor, K.Y.P. Apperley, Transglutaminase inhibitors: a patent review, Expert Opin. Ther. Pat. 26 (2016) 49–63, https://doi.org/10.1517/13543776.2016.1115836.
[31] J.-P. Renaud, C. Chung, U.H. Danielson, U. Egner, M. Hennig, R.E. Hubbard, H. Nar, Biophysics in drug discovery: impact, challenges and opportunities, Nat. Rev. Drug Discov. 15 (2016) 679–698, https://doi.org/10.1038/nrd.2016.123.
[32] A. Langer, P.A. Hampel, W. Kaiser, J. Knezevic, T. Welte, V. Villa, M. Maruyama, M. Svejda, S. Jähner, F. Fischer, R. Strasser, U. Rant, Protein analysis by time-resolved measurements with an electro-switchable DNA chip, Nat. Commun. 4 (2013), https://doi.org/10.1038/ncomms3099.
[33] A. Langer, W. Kaiser, M. Svejda, P. Schwertler, U. Rant, Molecular dynamics of DNA–protein conjugates on electrified surfaces: solutions to the drift-diffusion equation, J. Phys. Chem. B 118 (2014) 597–607, https://doi.org/10.1021/jp410640z.
[34] H. Thomas, K. Beck, M. Adamczyk, P. Aeschlimann, M. Langley, R.C. Oita, L. Thiebach, M. Hils, D. Aeschlimann, Transglutaminase 6: a protein associated with central nervous system development and motor function, Amino Acids 44 (2013) 161–177, https://doi.org/10.1007/s00726-011-1091-z.
[35] H. Elsässer, R. MacDonald, M. Dienst, H. Kern, Characterization of a transglutaminase expressed in human pancreatic adenocarcinoma cells, Eur. J. Cell Biol. 61 (1993) 321–328.
[36] S. Schaertl, M. Prime, J. Wityak, C. Dominguez, I. Munoz-Sanjuan, R.E. Pacifici, S. Courtney, A. Scheel, D. Macdonald, A profiling platform for the characterization of transglutaminase 2 (TG2) inhibitors, J. Biomol. Screen 15 (2010) 478–487, https://doi.org/10.1177/1087057110366035.
[37] R. Király, É. Csősz, T. Kurtán, S. Antus, K. Szigeti, Z. Simon-Vecsei, I.R. Korponay-Szabó, Z. Keresztessy, L. Fésüs, Functional significance of five noncanonical Ca^{2+}-binding sites of human transglutaminase 2 characterized by site-directed mutagenesis: Ca^{2+}-binding sites of TG2, FEBS J. 276 (2009) 7083–7096, https://doi.org/10.1111/j.1742-4658.2009.07420.x.
[38] K.E. Achyuthan, C.S. Greenberg, Identification of a guanosine triphosphate-binding site on Guinea pig liver transglutaminase, J. Biol. Chem. 262 (1987) 1901–1906.
[39] Y. Takeuchi, P.J. Birckbichler, M.K. Patterson, K.N. Lee, Putative nucleotide binding sites of Guinea pig liver transglutaminase, FEBS Lett. 307 (1992) 177–180, https://doi.org/10.1016/0014-5793(92)80762-6.
[40] G.E. Begg, S.R. Holman, P.H. Stokes, J.M. Matthews, R.M. Graham, S.E. Iismaa, Mutation of a critical arginine in the GTP-binding site of transglutaminase 2 disinhibits intracellular cross-linking activity, J. Biol. Chem. 281 (2006) 12603–12609, https://doi.org/10.1074/jbc.M600146200.
[41] A.S. Raw, D.E. Coleman, A.G. Gilman, S.R. Sprang, Structural and Biochemical characterization of the GTPγS-, GDP.P_i-, and GDP-bound forms of a GTPase-deficient Gly^{42} to val mutant of $G_{i\alpha1}$, Biochemistry 36 (1997), https://doi.org/10.1021/bi971912p 15660–0.
[42] Q. Ruan, J. Tucholski, S. Gundemir, The differential effects of R580A mutation on transamidation and GTP binding activity of rat and human type 2 transglutaminase, Int. J. Clin. Exp. Med. 1 (2008) 248–259.
[43] S.K. Oteng-Pabi, C. Pardin, M. Stoica, J.W. Keillor, Site-specific protein labelling and immobilization mediated by microbial transglutaminase, Chem. Commun. 50 (2014) 6604–6606, https://doi.org/10.1039/C4CC00994K.
[44] W. Steffen, F.C. Ko, J. Patel, V. Lyamichev, T.J. Albert, J. Benz, M.G. Rudolph, F. Bergmann, T. Streidl, P. Kratzsch, M. Boenitz-Dulat, T. Oelschlaegel, M. Schraeml, Discovery of a microbial transglutaminase enabling highly site-specific labeling of proteins, J. Biol. Chem. 292 (2017) 15622–15635, https://doi.org/10.1074/jbc.M117.797811.
[45] C.S. Theile, M.D. Witte, A.E.M. Blom, L. Kundrat, H.L. Ploegh, C.P. Guimaraes, Site-specific N-terminal labeling of proteins using sortase-mediated reactions, Nat. Protoc. 8 (2013) 1800–1807, https://doi.org/10.1038/nprot.2013.102.
[46] P.J. Tonge, Drug–target kinetics in drug discovery, ACS Chem. Neurosci. 9 (2018) 29–39, https://doi.org/10.1021/acschemneuro.7b00185.
[47] S.R.J. Hoare, B.A. Fleck, J.P. Williams, D.E. Grigoriadis, The importance of target binding kinetics for measuring target binding affinity in drug discovery: a case study from a CRF1 receptor antagonist program, Drug Discov. Today (2019), https://doi.org/10.1016/j.drudis.2019.09.011 S1359644619303551.

Abbreviations

TG2: transglutaminase 2, tissue transglutaminase
Z-DON: benzyloxycarbonyl-(6-diazo-5-oxonorleucinyl)-L-valinyl-L-prolinyl-L-leucinmethylester
GMP: Guanosine 5′-monophospate disodium salt hydrate
GDP: guanosine 5′-diphosphate sodium salt
GTP: guanosine 5′-triphosphate sodium salt
GTPγS: guanosine 5′-O-(3-thiotriphosphate)
EDTA: ethylenediaminetetraacetic acid
EGTA: ethylene glycol-bis(β-aminoethyl ether)-N,N,N′,N'-tetraacetic acid
TCEP: tris(2-carboxyethyl)phosphine)
k_{on}: association rate constant
k_{off}: dissociation rate constant
K_D: dissociation constant
D_H: hydrodynamic diameter